9. THE 2015 EXTREME DROUGHT IN WESTERN CANADA

Kit Szeto, Xuebin Zhang, Robert Edward White, and Julian Brimelow

Analysis results indicate that the 2015 extreme drought in western Canada was likely an outcome of anthropogenically influenced warm spring conditions and naturally forced dry weather from May to July.

Introduction. Although drought is common over western Canada (Bonsal et al. 2011), the drought that affected the area during the spring and summer of 2015 (Fig. 9.1a) was unusual in terms of its severity, extent, and impacts. British Columbia (B.C.) and Alberta were the most severely affected provinces. Vast areas in southern B.C. were assigned the highest possible (Level-4) drought rating by the B.C. government, several extreme-low streamflow advisories, and extreme wildfire risk ratings. Stringent water restrictions were in place by the end of June (AFCC 2016). In Alberta, conditions were even drier, and the Alberta government declared the province an Agricultural Disaster Area by early August. The extreme dry and warm conditions also created one of the most active and longest wildfire seasons for western Canada, and some rivers ran at their lowest recorded flows since measurements began 80 to 100 years ago (CMOS 2016). The extreme heat and dryness the region experienced in 2015 have raised concerns as to whether or not anthropogenic climate change (ACC) has increased the risk of extreme droughts in the area; this is the question we attempt to address in this paper.

Hydrometeorological conditions. Because the drought affected a vast area that includes regions characterized by different climate conditions, this study focuses on southern B.C., among the worst-affected regions. Three critical factors need to exist for severe drought to occur in southern B.C.: 1) low snowpack near the end of winter, 2) dry spring (May–June), and 3) dry summer (July–August) conditions (BCMOE 2016). The winter preceding the drought was characterized by near-normal precipitation. Apart from the extremely low snowpack that was observed in southwestern B.C. throughout the winter, near-normal to slightly below-normal snowpacks were present near the end of winter across most of the province (BCRFC 2015a). However, due to anomalously warm temperatures in March and April (MA; Fig. 9.2a), record low snow water equivalent (SWE) was observed over most of southern B.C. by 1 May (BCRFC 2015b). A persistent upper ridge off the west coast of North America (Fig. 9.1b) resulted in extraordinary warm and dry conditions from May through July (MJJ; Fig. 9.1c). The low SWE was compounded by the extreme dry conditions to create one of the worst droughts in the region. Time series of region-averaged standardized precipitation and evapotranspiration index (SPEI; Vicente-Serrano et al. 2010) for MJJ shows that the value for 2015 was the second lowest for the 1950–2015 period (Fig.9.1d), reflecting the significant surface moisture deficit in the area.

Methods. Attribution for the 2015 event is carried out using CMIP5 results (Taylor et al. 2012). It is well-known that coarse-grid climate models have very limited skills in simulating precipitation or SWE at regional scales. The preceding discussion suggests that it is justifiable to simplify the attribution analysis by limiting the drivers to the warm MA temperature (T_{34}) that caused the enhanced and earlier than normal melt and subsequent low summer runoff, and the hot and dry MJJ weather that aggravated the conditions during the growing season. In addition, the intensity of the upper ridge, which is physically linked to the variability of both precipitation (P) and temperature (T) during MJJ, is used as proxy for both variables.

It is evident from the point correlation map of region-averaged MJJ P with geopotential heights (Z) at 500 hPa (Fig. 9.1e) that dry (wet) conditions are related to positive (negative) upper-level height anomalies off the west coast. A parameter (H) is formulated to quantify the intensity of the upper-level ridge (see

AFFILIATIONS: Szeto, Zhang, and White—Environment and Climate Change Canada, Downsview, Ontario, Canada; Brimelow—Environment and Climate Change Canada, Edmonton, Alberta, Canada

DOI:10.1175/BAMS-D-16-0147.1

A supplement to this article is available online (10.1175/BAMS-D-16-0147.2)

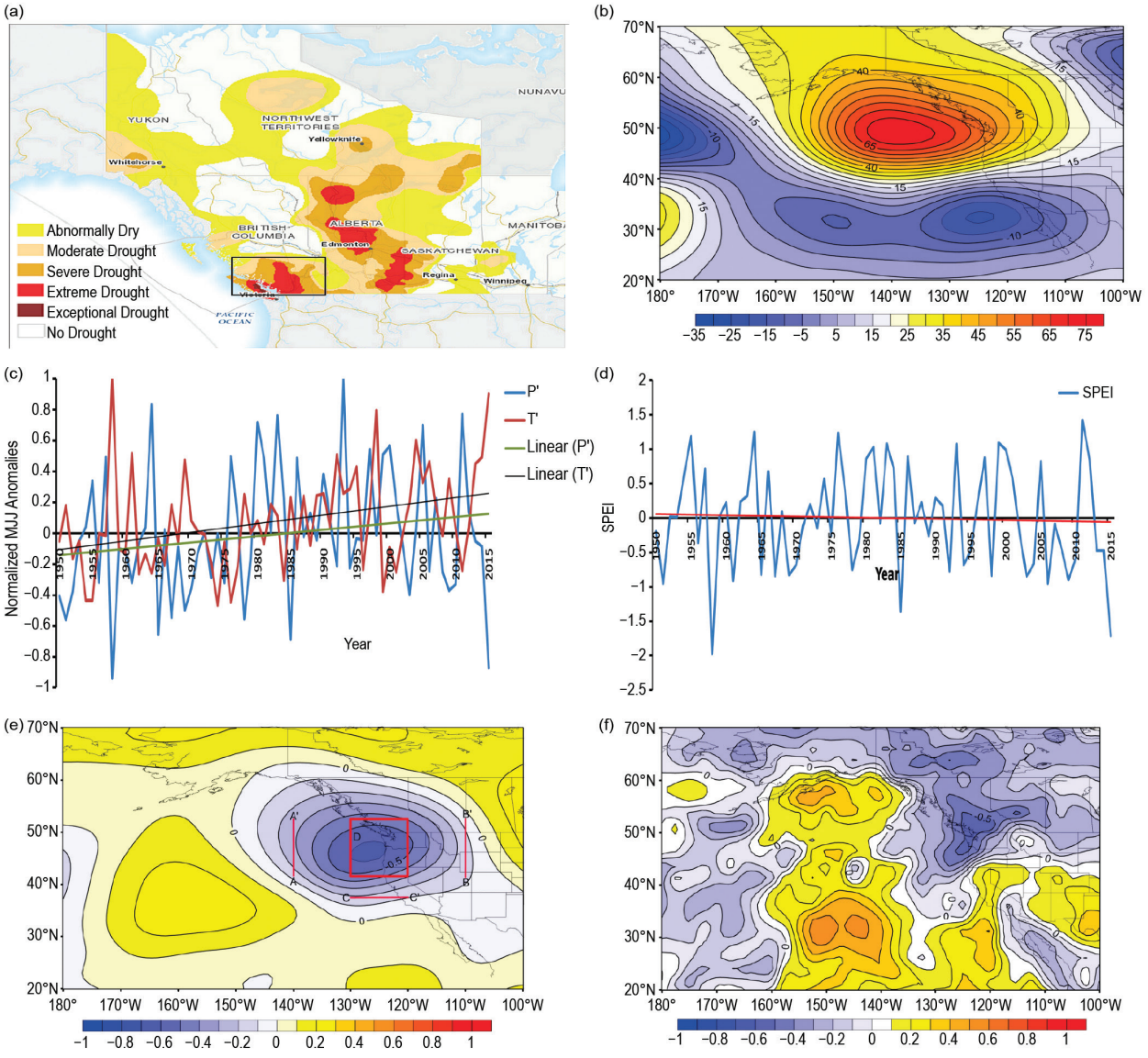

Fig. 9.1. (a) Jul 2015 drought conditions over western Canada (adapted from AAFC 2016). The rectangle over southern B.C. shows the study area where spatial averages of parameters are calculated. (b) MJJ height anomalies at 500 hPa from NCEP reanalysis (Kalnay et al. 1996). (c) 1950–2015 time series of normalized area-average MJJ precipitation and temperature anomalies computed from Environment and Climate Change Canada's homogenized CANGRD monthly dataset (Vincent et al. 2015). (d) Time series (blue) and linear trend (red) of area-average MJJ SPEI obtained from the SPEI Global Drought Monitor (http://sac.csic.es/spei/map/maps.html). (e) Map of correlations between the P' time series in (b) and MJJ NCEP height at 500 hPa. Also shown are the region D and cross-sections used in the computation of H with Eq. (1). (f) Map of correlations between the time series of H computed from NCEP reanalysis with MJJ GPCP precipitation (Adler et al. 2012).

the online supplemental information for details):

$$H = 3\langle Z' \rangle_D - \langle Z' \rangle_{AA'} - \langle Z' \rangle_{BB'} - \langle Z' \rangle_{CC'} \quad (1)$$

where the anomalies are relative to the 1971–2000 climatology. Locations of the region D and transects used in the calculation of H are shown in Fig. 9.1e. H exhibits statistically significant correlations with precipitation over western Canada in general (Fig. 9.1f). Contemporaneous correlations between detrended H and P, T, and SPEI averaged over southern B.C. are −0.68, 0.74, and −0.76, respectively. Time series of H computed from reanalysis data (Fig. 9.2c) shows that years of extreme positive values of H (e.g., above the 95th percentile—Hc = 60 m) also correspond well with extreme dry and warm years. In particular, both the driest and hottest MJJ and largest H occurred in 1958, and the value for 2015 is the third

largest over the period. The other two high *H* years (1969 and 1992) were also exceptionally warm and dry, but the conditions improved in July, resulting in less extreme seasonal averages.

To determine how greenhouse gas (GHG) forcing influences T_{34} and the *H*-index, we compare the trends and other statistics of these variables as computed from observed or reanalysis data and ensembles of CMIP5 historical simulations with natural (NAT) or all (ALL) forcings. The list of 19 CMIP5 models used in the analysis is given in the online supplemental information. The change in likelihood of extreme droughts in southern B.C. from GHG forcing is assessed by evaluating how the exceedance probabilities for these variables differ between the ALL and NAT ensembles. This is achieved by calculating the fraction of attributable risk (FAR; Allen 2003), as detailed in the supplemental information.

Results. We first investigate if ACC has increased the risk of reduced snowpacks at the end of winter. There is no detectable trend of December–March precipitation in either the observations or CMIP5 results (not shown). There are, however, significant warming trends for T_{34} in both the observed and CMIP5-ALL ensemble-mean data, but not for the NAT runs (Fig. 9.2a). No significant increasing trend is evident in the ensemble maximum T_{34} for either ALL or NAT. The best estimate (median) FAR calculated by using thresholds corresponding to the 96th percentiles of

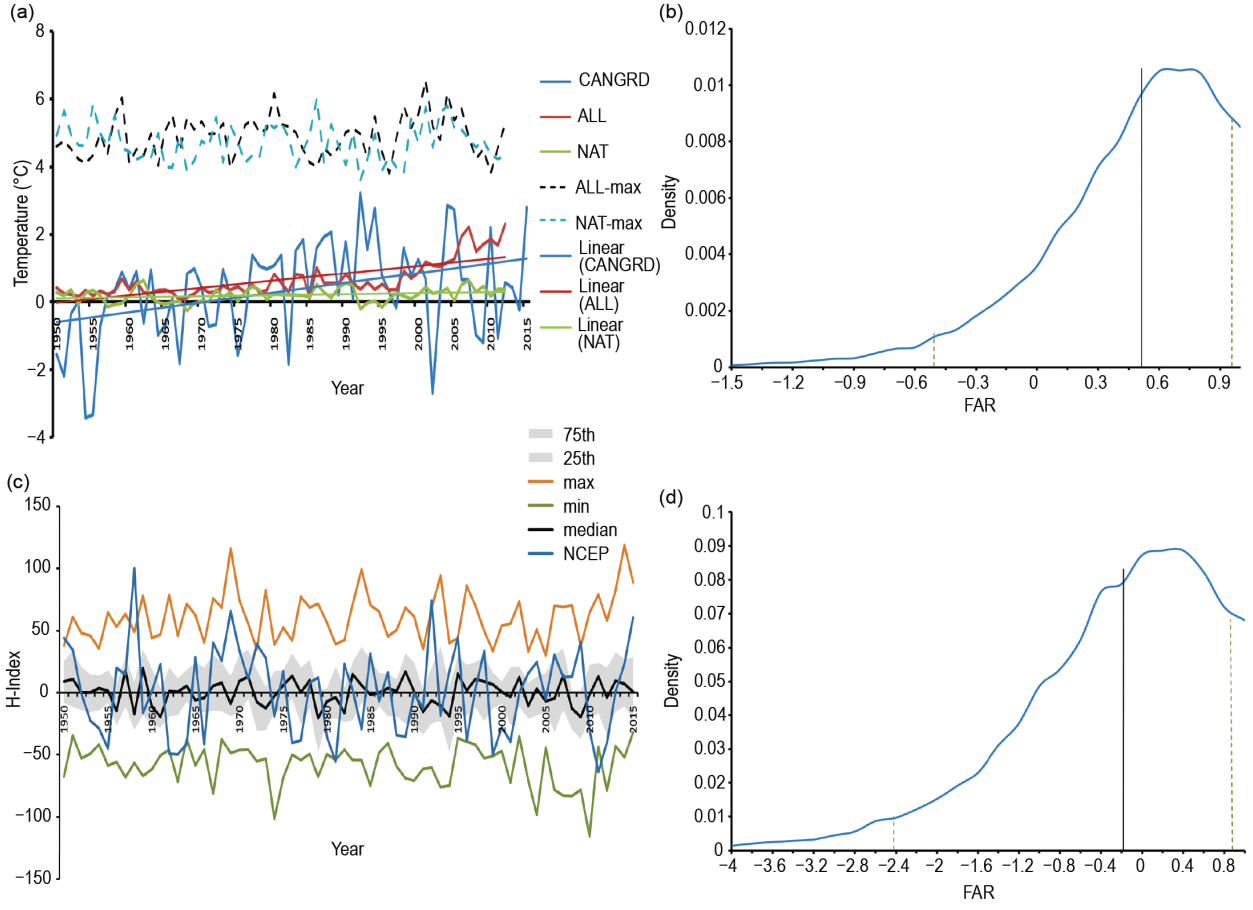

Fig. 9.2 (a) Time series of MA temperatures (T_{34}) computed from CANGRD (blue) dataset and the ensemble mean T_{34} for experiments ALL (red) and NAT (green), along with linear trends for the corresponding series. Also shown are the time series of ensemble maximum for ALL (dashed black) and NAT (blue dashed). (b) Empirical distribution of FAR computed with thresholds set as the 96th percentiles of T_{34} from the individual ALL runs. (c) 1950–2015 time series of the MJJ *H*-index computed from NCEP reanalysis (blue) and the ensemble minimum (green), median (black), and maximum (orange) of *H* for experiment ALL. Gray shading indicates the range between the 25th and 75th percentiles. The CMIP5 historical simulations end at 2005 and ensemble statistics for *H* from 2006 to 2015 are computed from the RCP4.5 projection results. (d) As in (b) but for the MJJ *H*-index and computed with thresholds set as the 96th percentiles of *H* from the ALL runs.

T34 in ALL runs (i.e., the same percentile for the T_{34} observed for 2015) is about 0.49 (Fig. 9.2b). This suggests that external forcing (mainly anthropogenic forcing) may have doubled the risk for the occurrence of the recent extreme high T_{34} that resulted in the early snowmelt, as evidenced by the early peak flows in the streamflow data (BCRFC 2015b). We note, however, that the FAR estimate has a large spread.

How ACC might have affected the MJJ conditions is examined next. Figure 9.1c shows that both *T* and *P* increased between 1950 and 2015. Given that there is no trend in the area-average SPEI (Fig. 9.1d), it is likely that the effects of increasing *P* on surface water balance could have been offset by the increase in evapotranspiration due to the warming temperatures during this time. Regardless of whether the increases in *T* and *P* were the result of ACC, the results suggest they currently do not have detectable influence on surface water balance in MJJ and thus drought risk in the region.

Next we assess whether GHG forcing has affected the upper ridge that creates the meteorological conditions (i.e., low *P* and high *T*) that are critical for the development of extreme drought. The bounds of *H* computed from either the ALL or NAT ensembles are comparable to those exhibited in the *H*-index derived from the NCEP reanalysis, suggesting that the "observed" variability of *H* was reproduced by the models in these two experiments. No significant trend (at 5% level) is detected for either the NCEP *H* or ensemble statistics (median, extrema, etc.) for the two CMIP5 experiments (Fig. 9.2c; results are not shown for NAT), suggesting that GHG forcing has not produced detectable change in the intensity of the west coast upper ridge and the attendant increase in the risk of drought in the area.

Lastly, we examine if ACC has increased the risk of extreme *H* that are associated with extreme droughts. Results show that the exceedance probability for extreme *H* in ALL runs is similar to and perhaps somewhat smaller than that in NAT runs (Fig. 9.2d), suggesting that GHG forcing has not resulted in detectable increase in the risk of extremely high *H*, and consequently the occurrence of intense stationary upper ridge and associated extreme warm and dry conditions. Similar results are also obtained for a parallel analysis that was carried out by constructing *H* based on the *Z*' composited over the three driest MJJ during the 1950–2015 period.

Concluding remarks. The multifaceted characteristics and forcings of droughts render attribution analysis of their causes a challenging task, particularly for a region where both cold- and warm-season processes are critical for drought development. Results from this study indicate that ACC likely played a role in causing the warm late-winter temperatures and the associated reduction in snowpack that set the stage for the 2015 drought. On the other hand, there is no detectable evidence that GHG forcing influenced the intensity or the likelihood of occurrence for the strong and persistent upper-air ridge off the west coast that brought the record heat and dryness in MJJ, which escalated the drought to an extreme event. The results thus suggest that the extreme drought was likely an outcome of anthropogenic effect that has increased the occurrence of extreme warm spring temperatures and natural climate variability that caused the persistent upper ridge. The climate of western Canada is known to be influenced strongly by key Pacific climate variability modes on sub-seasonal to multidecadal time scales (Gan et al. 2007). For instance, the developing intense 2015–16 El Niño could have contributed to the extreme summer conditions. However, the question of whether or not El Niño played a role does not alter the conclusion that the extreme MJJ conditions were mainly a result of natural variability. Lastly, it is noteworthy that analysis of CMIP5 projections suggests that both late-winter warming and the west coast upper ridge could be enhanced in response to GHG forcing during the latter part of this century. As such, effects of changes in warm-season precipitation and temperature on the surface water budget might not offset each other, or may even reinforce each other in the future. The collective effects of these projected changes on future extreme droughts in western Canada are being investigated and the results will be reported elsewhere.

ACKNOWLEDGEMENTS. We thank the three anonymous reviewers and Dr. James Kossin for helpful comments. This research is supported by Environment and Climate Change Canada and the Changing Cold Regions Network (CCRN) which is sponsored by the Natural Sciences and Engineering Research Council of Canada (NSERC).

REFERENCES

AAFC, 2016: 2015 Annual review of agroclimate conditions across Canada. Agriculture and Agri-Food Canada , 23 pp. [Available online at www.agr.gc.ca/resources/prod/doc/pdf/agroclimate_ar_2015-en.pdf.]

Adler, R. F., G. Gu, and G. Huffman, 2012: Estimating climatological bias errors for the Global Precipitation Climatology Project (GPCP). *J. Appl. Meteor. Climatol.*, **51**, 84–99, doi:10.1175/JAMC-D-11-052.1.

Allen, M., 2003: Liability for climate change. *Nature*, **421**, 891–892, doi:10.1038/421891a.

BCMOE, 2016: British Columbia drought response plan. B.C. Ministry of Environment, 38 pp. [Available online at http://www2.gov.bc.ca/assets/gov/environment/air-land-water/water/drought-info/drought-response-plan-update-june-2015.pdf.]

BCRFC, 2015a: Water supply and snow survey bulletin: March 1, 2015. British Columbia River Forecast Centre [Available online at http://bcrfc.env.gov.bc.ca/bulletins/watersupply/archive.htm.]

——, 2015b: Water supply and snow survey bulletin: May 1, 2015. British Columbia River Forecast Centre [Available online at http://bcrfc.env.gov.bc.ca/bulletins/watersupply/archive.htm.

Bonsal, B. R., E. Wheaton , A. C. Chipanshi , C. A. Lin, D. J. Sauchyn, and L. Wen, 2011: Drought research in Canada: A review. *Atmos.—Ocean*, **49**, 303–319, doi:10.1080/07055900.2011.555103.

CMOS, 2016: Canada's top ten weather stories for 2015. Canadian Meteorological and Oceanographic Society. [Available online at www.cmos.ca/site/top_ten?a=2015.]

Gan, T., A. Gobena, and Q. Wang, 2007: Precipitation of southwestern Canada: Wavelet, scaling, multifractal analysis and teleconnection to climate anomalies. *J. Geophys. Res.*, **112**, D10110, doi:10.1029/2006JD007157.

Kalnay, E., and Coauthors, 1996: The NCEP/NCAR 40-Year Reanalysis Project. *Bull. Amer. Meteor. Soc.*, **77**, 437–470.

Taylor, K. E., R. J. Stouffer, and G. A. Meehl, 2012: An overview of CMIP5 and the experiment design. *Bull. Amer. Meteor. Soc.*, **93**, 485–498, doi:10.1175/BAMS-D-11-00094.1.

Vicente-Serrano, S. M., S. Beguería, and J. I. López-Moreno, 2010: A multiscalar drought index sensitive to global warming: The standardized precipitation evapotranspiration index. *J. Climate*, **23**, 1696–1718, doi:10.1175/2009JCLI2909.1.

Vincent, L.A., X. Zhang, R. D. Brown, Y. Feng, E. Mekis, E. J. Milewska, H. Wan, and X. L. Wang, 2015: Observed trends in Canada's climate and influence of low-frequency variability modes. *J. Climate*, **28**, 4545–4560. doi:10.1175/JCLI-D-14-00697.1.